Accepted Manuscript

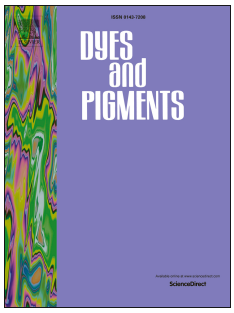

Unique fluorescence of boronic acid derived salicylidenehydrazone complexes with two perpendicular ICT: Solvent effect on PET process

Boyu Zhang, Shichao Wang, Jingyun Tan, Xuanjun Zhang

PII: S0143-7208(18)30327-9

DOI: 10.1016/j.dyepig.2018.03.046

Reference: DYPI 6631

To appear in: *Dyes and Pigments*

Received Date: 10 February 2018

Revised Date: 14 March 2018

Accepted Date: 23 March 2018

Please cite this article as: Zhang B, Wang S, Tan J, Zhang X, Unique fluorescence of boronic acid derived salicylidenehydrazone complexes with two perpendicular ICT: Solvent effect on PET process, *Dyes and Pigments* (2018), doi: 10.1016/j.dyepig.2018.03.046.

Graphical Abstracts

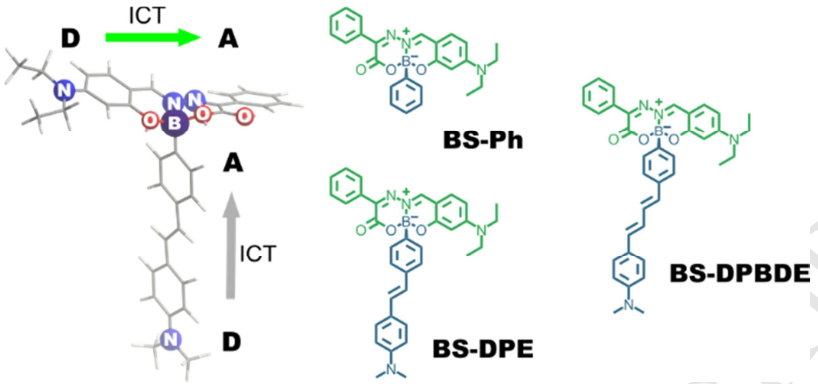

Unique fluorescence of boronic acid derived salicylidenehydrazone complexes with two perpendicular ICT: solvent effect on PET process

Boyu Zhang, Shichao Wang, Jingyun Tan, Xuanjun Zhang*

Faculty of Health Sciences, University of Macau, Macau SAR, China.

Email: xuanjunzhang@umac.mo

Abstract: Solvent effects on the absorption and emission spectra of organic compounds have been widely observed. It is usually found that the positions, intensities and shapes of its bands are usually modified by these solvents. The solvent effects on intramolecular charge transfer (ICT) process have been extensively reported, whereas the solvent effect on photoinduced electron transfer (PET) process is scarce. In this contribution, it was disclosed that boronic acid derived salicylidenehydrazone complexes (BSs), BS-DPE and BS-DPBDE, with two perpendicular ICT states developed a non-fluorescent PET compounds through separating its two ICT states by boron node. Relative strong acidic proton in non-hydrogen-bond accepting solvent were proved to actuate the vanishment of PET and reinstatement of its fluorescence.

Keywords: Solvent effects; Boronic acid; Salicylidenehydrazone; Photoinduced electron transfer; T-shaped molecular geometry

1. Introduction

Solvent effects[1, 2] have been widely observed in different areas of chemistry such as catalysis,[3] biochemistry[4] and photochemistry.[5] Of these observation, most concern its effects on the position of chemical equilibria and/or the rates of chemical reactions. Furthermore, from a photophysical point of view, the ground and excited state of solvated chromophore-containing molecules in different solvents might undergo a physical perturbation as compared with its isolated ones (gas state)[1]. Vibrational relaxation of electronic state with surrounding solvent are coincided with energy loss both from Franck-Condon excited (ground) state to equilibrium excited (ground) state, leading to Stokes shift.[6] Many types of positive, negative and inverted fluorosolvatochromistic dyes have been synthesized and widely applied in bioimaging and biosensing,[7] such as studying lipid domains,[8] apoptosis and endocytosis.[9] The theory of solvent effects on the fluorescence assumes that the fluorophore is a point dipole residing in the centre of a spherical cavity in a homogeneous and isotropic dielectric, which is so-called Lippert-Mataga theory[10] but deviated from authentic condition. Therefore, it is of paramount importance to come up with and fully comprehend specific fluorophores solute/solvent interaction, especially involving hydrogen bonding, electron-pair donor/electron-pair acceptor interactions or others.[1, 11, 12]

Over the last few years were recognized a special solvent effect on ground-state reversible isomerization of silica-rhodamines (SiR),[13] in which SiR-carboxyl exists predominantly in its spirolactone form in dioxane-water mixtures of dielectric constant less than 30. This seminal fluorogenic behaviour enabled multicolour imaging of target proteins in wash-free conditions.[14] Also, based on a hypothesis which proposed that the break of fluorophore-solvent hydrogen bond in the excited state account for fluorescence quenching,[15, 16] flavones-based fluorophores with carbonyl as hydrogen bond acceptors were demonstrated to be ideal wash-free bioprobe for mitochondria[17] and endoplasmic reticulum imaging.[18] Our group also recently found that boronic acid derived salicylidenehydrazone complexes (BSs) were ideal candidates for wash-free fluorescence imaging of cellular organelles.[19] A remarkably hypsochromic shift of intramolecular

charge-transfer (ICT) absorption band in water was observed than in apolar solvent, which were attributed to lower the n-state energy of oxygen lone pairs of the carbonyl group through hydrogen bonding with water.

In this contribution, we report that a peculiar fluorescence turn-on property of two BSs involved donor-acceptor diphenylpolyenes[20-22] as auxochrome. The versatile fluorescent dye platform BSs were first reported last year, which were constructed from modular assembly of boronic acids with schiff base ligand salicylidenehydrazone by groups of Goris and Pischel.[23] Subsequently, they thoroughgoingly explored the photophysical scope of the dyes through the variation of both the push-pull ICT character at the ligand backbone and the electronic nature of the boronic acid derived moiety, the latter of which have been demonstrated to be no influence on the Uv-vis absorption and fluorescence properties.[24] The T-shaped molecular geometry of BSs sparked our imagination on what photophysical properties will come into view if two perpendicular ICT states were located in BSs (**Scheme 1**). To the extent of our knowledge, there has been little research on fluorophore with this type molecular architecture.[25]

2. Experimental

2.1 General Information

All reagents were purchased from Aldrich or ShenZhen Dieckmann Technology Development co., LTD and were used without further purification, unless otherwise stated. HPLC grade solvent were used in Uv-vis and fluorescence studies. Uv-vis spectra were recorded on a SHIMADZU Uv-1800 spectrophotometer, with a quartz cuvette (path length 1 cm). The fluorescence spectra were recorded with a HORIBA Fluorolog$^{@}$-3 spectrofluorimeter. ^{1}H and ^{13}C NMR spectra were recorded on a BRUKER instrument (400 MHz and 100 MHz, respectively) and internally referenced to tetramethylsilane signal or residual protio solvent signals. Data for ^{1}H NMR are recorded as follows: chemical shift (δ, ppm), multiplicity (s, singlet; d, doublet; t, triplet; q, quartet; m, multiplet), intergration, coupling constant (Hz). Data for ^{13}C NMR are reported in terms of chemical shift (δ, ppm). High resolution mass spectra for all the new compounds were done by an

a Xevo G2-XS QTof spectrometer (Waters, USA). The fluorescence quantum yields (QYs) were quantified using Fluorescein as the standard (Φ_f = 0.89, in 0.1 M NaOH). The QYs can be calculated through adopting the following equation:

$$\Phi_s = \Phi_r(A_r n_s^2 F_s)/(A_s n_r^2 F_r)$$

where the subscripts s and r denote the sample and the standard (Fluorescein), respectively, Φ is the quantum yield, F is the integrated emission intensity, A is the absorbance, and n is the refractive index.

Fluorescence lifetimes were detected by a DeltaTime™ TCSPC on Fluorolog®. The monitored wavelength was 545 nm. Fluorescence decay histograms were recorded using the time-correlated single photon counting technique in 4095 channels through a HORIBA Fluorolog$^{@}$-3 spectrofluorimeter equipped with a HORIBA NanoLED source (N-455 nm). Histograms of the instrument response functions and sample decays were obtained until it typically reached 1.0×10^4 counts. The fitting parameters (decay times and pre-exponential factors) were decided by minimizing the reduced chisquare χ^2.

For a two-exponential decay the average lift time is given by following equation:

$$\bar{\tau} = \frac{\alpha_1\tau_1^2 + \alpha_2\tau_2^2}{\alpha_1\tau_1 + \alpha_2\tau_2}$$

The time-dependent density functional theory (TD-DFT/B3LYP) calculations of BS-DPE, BS-DPBDE were performed. All calculations were performed with the G03 software. The TD-DFT calculation of the lowest 25 singlet-singlet excitation energies was calculated with a basis set composed of 6-31G (d, p) for C, N, H, O, B atoms. The lowest 25-spin allowed singlet-singlet transitions, up to the energy of about 5 eV, were taken into account for the calculation of the absorption spectra.

2.2 Synthesis

(Z)-2-(((E)-4-(diethylamino)-2-hydroxybenzylidene)hydrazono)-2-phenylacetic acid (Ligand) (Scheme 2-1). Adopting a literature procedure with some reasonable modification,[23]

hydrazonoe (2.5 mmol, 490 mg) was completely dissolved in 5 mL water firstly and 20 mL methanol was added. After shaking moderately, this solution was eluted through a columned packed with Amberlyst@ 15 (5 g wet resin exchanged with 10 mL methanol for three times) and dropped into a methanolic solution of SA (2.5 mmol, 483 mg in 5 mL methanol). The ultimate solution was stirred for 2 h at room temperature and then incubation at 4 □ in refrigerator overnight. The slurry was filtered and washed with cold methanol (5 mL) three times, and afterwards collected as orange powder: yield 65%; ^{1}H NMR (400 MHz, $CDCl_3$) δ 8.16 (s, 1H), 8.09 – 8.01 (m, 2H), 7.71 (d, *J* = 2.3 Hz, 1H), 7.43 (td, *J* = 7.0, 5.8, 3.0 Hz, 3H), 7.19 (d, *J* = 9.2 Hz, 1H), 6.36 (dd, *J* = 9.2, 2.3 Hz, 1H), 3.59 (q, *J* = 7.1 Hz, 4H), 1.31 (t, *J* = 7.1 Hz, 6H). ^{13}C NMR (101 MHz, DMSO-d6) δ 167.3, 164.9, 161.9, 159.5, 152.4, 134.7, 131.9, 131.7, 129.6, 127.3, 106.5, 104.9, 97.3, 44.5, 13.0. HRMS-ESI calcd for $C_{19}H_{22}N_3O_3$ ($[M+H]^+$), 340.1661; found, 340.1703.

(4-boronobenzyl)triphenylphosphonium bromide. A solution containing (4-(bromomethyl)phenyl)boronic acid (5.2 mmol, 1.12 g) and triphenylphosphane (5.72 mmol, 1.5 g) in 160 mL MeCN was refluxed for 12 h. After the completion of reaction, the solvent was removed in vacuo and the residue was triturated with diethyl ether (3 × 10 mL) and collected as white precipitate: yield 95%; 1H NMR (400 MHz, DMSO-d_6) δ 7.88 – 7.78 (m, 3H), 7.71 – 7.51 (m, 17H), 6.90 (dd, J = 8.1, 2.5 Hz, 2H), 4.98 (d, J = 15.4 Hz, 2H). ^{13}C NMR (101 MHz, DMSO-d_6) δ 135.6, 135.6, 134.9, 134.8, 134.6, 134.5, 130.6, 130.5, 130.4, 130.4, 118.7, 117.9, 29.0. HRMS-ESI calcd for $C_{25}H_{23}BO_2P$ ($[M-Br]^+$), 397.1523; found, 397.1613.

8-(diethylamino)-2,5-diphenyl-3H,5H-5l4,12l4-benzo[5,6][1,3,2]oxazaborinino[2,3-b][1,3,4,2]oxadiazaborinin-3-one (BS-Ph) (Scheme 2-4). The derivate of phenylboronic acid (0.3 mmol) was dissolved in CH_3CN (3 mL), toward which the ligand (0.33 mmol, 112 mg) was added. The resulting solution was refluxed until the termination of reaction. And then, the solution was concentrated and the residue was triturated with cold methanol for washing away minor impurities. [19]Orange solid; Yield 95%; ^{1}H NMR (400 MHz, $CDCl_3$) δ 8.21 (s, 1H), 7.96 – 7.88 (m, 2H), 7.41 – 7.27 (m, 5H), 7.18 – 7.08 (m, 4H), 6.29 (dd, J = 9.1, 2.4 Hz, 1H), 6.13 (d, J = 2.3

Hz, 1H), 3.37 (ddt, J = 16.6, 14.8, 7.4 Hz, 4H), 1.16 (t, J = 7.2 Hz, 6H). ^{13}C NMR (101 MHz, CDCl3) δ 161.6, 157.3, 155.8, 154.0, 153.6, 134.6, 132.7, 130.8, 130.8, 129.5, 128.2, 127.8, 127.6, 107.7, 106.4, 98.7, 45.4, 12.8. HRMS-ESI calcd for $C_{25}H_{25}BN_3O_3$ ([M+H]$^+$), 426.1989; found, 426.1873.

(E)-8-(diethylamino)-5-(4-(4-(dimethylamino)styryl)phenyl)-2-phenyl-3H,5H-5l4,12l4-benzo[5,6][1,3,2]oxazaborinino[2,3-b][1,3,4,2]oxadiazaborinin-3-one (BS-DPE) (Scheme 2-5). (E)-(4-(4-(dimethylamino)styryl)phenyl)boronic acid in Scheme 2-2 was synthesized on the previous reports (Spectroscopic sugar sensing by a stilbene derivative with push (Me_2N-)-pull ($(HO)_2B$-)-type substituents). The derivate of phenylboronic acid (0.3 mmol) was dissolved in CH_3CN (3 mL), toward which the ligand (0.33 mmol, 112 mg) was added. The resulting solution was refluxed until the termination of reaction. And then, the solution was concentrated and the residue was dissolved in tiny amount toluene and then purified by column chromatography (Hexane : EtOAc=10:1). Pale orange solid: yield 65%. ^{1}H NMR (400 MHz, Chloroform-*d*) δ 8.31 (s, 1H), 8.07 – 7.99 (m, 2H), 7.51 – 7.30 (m, 9H), 7.24 (d, *J* = 9.1 Hz, 1H), 6.98 (d, *J* = 16.3 Hz, 1H), 6.85 (d, *J* = 16.2 Hz, 1H), 6.78 – 6.66 (m, 2H), 6.39 (dd, *J* = 9.1, 2.4 Hz, 1H), 6.24 (d, *J* = 2.3 Hz, 1H), 3.46 (ddt, *J* = 23.8, 14.5, 7.0 Hz, 4H), 2.98 (s, 6H), 1.26 (t, *J* = 7.2 Hz, 6H). ^{13}C NMR (101 MHz, $CDCl_3$) δ 161.6, 157.3, 155.8, 154.1, 153.5, 150.0, 137.6, 134.5, 132.7, 131.1, 130.8, 129.5, 128.2, 128.1, 127.4, 126.1, 125.3, 124.8, 112.5, 107.7, 106.4, 98.7, 45.4, 40.5, 12.7. HRMS-ESI calcd for $C_{35}H_{36}BN_4O_3$ ([M+H]$^+$), 571.2880; found, 571.2463.

8-(diethylamino)-5-(4-((1E,3E)-4-(4-(dimethylamino)phenyl)buta-1,3-dien-1-yl)phenyl)-2-phenyl-3H,5H-5l4,12l4-benzo[5,6][1,3,2]oxazaborinino[2,3-b][1,3,4,2]oxadiazaborinin-3-one (BS-DPBDE) (Scheme 2-6). The derivate of phenylboronic acid (0.3 mmol) was dissolved in CH_3CN (3 mL), toward which the ligand (0.33 mmol, 112 mg) was added. The resulting solution was refluxed until the termination of reaction. And then, the solution was concentrated and the residue was dissolved in tiny amount toluene and then purified by column chromatography (Hexane : EtOAc=10:1). Pale orange solid: yield 54%. ^{1}H NMR (400 MHz, Chloroform-*d*) δ 8.31 (s, 1H), 8.06 – 7.98 (m, 2H), 7.51 – 7.20 (m, 10H), 6.88 (dd, *J* = 15.3, 10.5 Hz, 1H), 6.81 – 6.66 (m, 3H), 6.54 (t, *J* = 16.1 Hz, 2H), 6.39 (dd, *J* = 9.2, 2.4 Hz, 1H), 6.24 (d, *J* = 2.4 Hz, 1H), 3.47

(qt, J = 14.4, 7.3 Hz, 4H), 2.98 (s, 6H), 1.27 (t, J = 7.0 Hz, 6H). ^{13}C NMR (101 MHz, $CDCl_3$) δ 161.6, 157.3, 155.8, 154.1, 153.5, 137.3, 134.5, 132.7, 132.6, 131.1, 130.8, 129.5, 129.4, 128.2, 127.4, 125.6, 125.4, 112.5, 107.6, 106.4, 98.7, 45.4, 40.5, 29.7, 12.7. HRMS-ESI calcd for $C_{37}H_{38}BN_4O_3$ ($[M+H]^+$), 597.3037; found, 597.2697.

3. Results and discussion

3.1 Synthesis

Two derivatives of diphenylethene (DPE) or diphenylbutadiene (DPBDE), possessing a dimethylamino and a boronic acid group as electron-donor and electron-withdrawing groups, were settled on assembly with Schiff base ligand to create targeted molecules, BS-DPE and BS-DPBDE. The B-N dative bond in BSs could furnish an extra molecular stability,[26] which might also modify the electronic properties of auxiliary ICT state. DPE-BA (boronic acid) and DPBDE-BA were synthesized by the Wittig reaction (**Scheme 2**) between the corresponding benzaldehydes and the para-boronic acid derivative of the benzyltriphenylphosphonium (TPP) bromide,[27] which were then converted into BS-DPE and BS-DPBDE by simple condensation with salicylidenehydrazone ligand.[23, 24]

3.2 Distinctive optical properties

Unexpectedly, light tangelo BS-DPE and BS-DPBDE are essentially nonfluorescent in the solid state (**Fig. 1**b) and show very weak fluorescence in chloroform (**Fig. 1**c), which is in marked contrast to BS-Ph with high fluorescence quantum yield (QY ca. 0.5-0.7) and brightness in chloroform as previous reports.[19, 23] Serendipitously, it was found BS-DPE and BS-DPBDE are highly luminescent in deuterated chloroform ($CDCl_3$) (**Fig. 1**d) during NMR test, in striking contrast to in chloroform. It spurred us into a detailed test on its absorption and emission spectra in different solvent.**Fig. 1**e shows that BS-DPE has a dual absorption band trait in nine selected solvents, where the low-energy band from 400 nm to 525 nm were attributed to ICT absorption of the ligand backbone, and the high-energy band within the range of 300 nm – 400 nm originated from ICT state of DPE.[20]

The spectra in $CDCl_3$ and HEPES buffer were unpredicted, the former of which shows a large hypsochromic shift of high-energy band from 357 nm to 320 nm in comparison with that in $CHCl_3$, the latter exhibits that both of bands broadened and stretched out to 410 nm and 550nm, indicating water molecules have obvious influence on both of ICT ground states. Our earlier report revealed that BS-Ph had just one local chromophore absorption band located at 400 nm, which is an outcome of interaction of backbone ICT state with water.[19] Based on the above facts in HEPES buffer, it could be concluded that the horizontal and vertical ICT states have independent features, but also interact with each other and offer an ensemble solvatochromism. Fluorescence spectra follow the same trend as the absorption spectra (**Fig. 1**f). High QY up to 0.43 was attained in $CDCl_3$, whereas no fluorescent signal was detected in HEPES. A red shift was observed in high polar solvent in comparison with apolar solvents (average 520 nm), up to 15 nm, 32 nm and 17 nm for PEG400, DMSO and CH_3OH, respectively. For BS-DPBDE, the spectral features are comparable to that of BS-DPE, but with three distinctions: (1) High energy-band is located at 344 nm for $CDCl_3$ and near 385 nm for others; (2) The intensities of high energy-band are higher than that of low energy-band in all solvents except $CDCl_3$; (3) The QY of BS-DPBD (0.52) is higher than BS-DPE in $CDCl_3$ (**Table 1**). Due to much higher brightness ($\varepsilon \times \Phi_s$) of BS-DPBDE, it was selected for further discussion.

3.3 Turn-on phenomena and characterization.

The extraordinary brightness in $CDCl_3$ made us think about the concealed factor in fluorescence turn-on. Hydrochloric acid as the main decomposed product of $CHCl_3$ was tested first.[28] As shown in **Fig. 2**a-b and Fig. S1-S2, the absorption and emission spectra of BS-DPBDE in different solvents were compared with that of corresponding solvent added HCl up to 15 uM. Distinctly, the spectral feature of BS-DPBDE in $CHCl_3$ with HCl was identical with that in $CDCl_3$, which indicates that it is easy for $CDCl_3$ to release DCl as acid for actuating fluorescence of BS-DPBDE. For other solvents with adding HCl, unexpectedly, there are no significant enhancement of fluorescence intensities even in apolar solvent toluene, and also no occurrence of high-energy absorption band blue-shift.

In toluene and THF, addition of HCl even caused the decrease in fluorescence a little bit. This fact points out that the fluorescent turn-on is not only an acid-actuation process, but also dependence on solvent. Next, the chloride solvents $C_2H_4Cl_2$ and CH_2Cl_2 were used to further investigate this solvent effect on fluorescence turn-on. From **Fig. 2**c, it can be seen that the low-energy band were heightened, and also that the low energy band lost its vibrational fine-structure when HCl was added into $CHCl_3$ and $C_2H_4Cl_2$, which are consonant with intensified fluorescence in $CHCl_3$ and $C_2H_4Cl_2$ with HCl (**Fig. 2**d). Afterwards, UV-vis and emission titration experiments of BS-DPBDE (10 μM) in $CHCl_3$ were recorded with increasing concentrations of HCl (**Fig. 2**e-f). The continuous addition of HCl from 1 uM to 20 uM induced a dramatic change in the spectra that accompanied two isosbestic points at 350 and 445 nm. The presence of an isosbestic point signified the presence of an equilibrium process between turn-on and turn-off states. No further spectral change was registered when HCl was added beyond the mole ratio of 1.25 equiv. The fluorescence intensity increase caused by addition of HCl to BS-DPBDE is linearly proportional to HCl concentration in the 1-7.5 uM range (**Fig. 2**f). Ensuingly, acetic acid, Trifluoroacetate (TFA) and sulfuric acid were selected for testing whether or not all acids could actuate the fluorescence of BS-DPBDE. **Fig. 2**g presents the fluorescence intensity change (I/I_0) upon adding acid into $CHCl_3$ solution, which manifest that acids with pKa lower than 3.0 enable the $CHCl_3$ solution of BS-DPBDE to be emitted. The spectral properties of BS-DPE were comparable with BS-DPBDE and the data were shown in Fig. S5.

Fluorescence decay parameters of the BS-DPBDE in different solvents without or with acids are listed in **Table 2**. Fluorescence decay profiles were satisfactorily fitted with a two-exponential model and lifetimes show apparent effect of solvent, much shorter lifetimes for polar solvent THF (1.23 ns) and DMSO (0.61 ns).[29] The faster component of the lifetime can be attributed to the ICT species, and the slower component is due to the presence of the LE molecules[30]. Remarkably, roughly twice prolongation of τ_1 were registered in $CHCl_3$ upon adding HCl and H_2SO_4 over others, especially in contrast to that

of TFA and acetic acid (**Fig. 3**a). It indicates that there might have some fresh species with longer lifetime, associated with high fluorescence. Schiff-base backbone and two dialkylamino-group confused us as to whether BS-DPBDE was degraded and which dialkylamino base group was vulnerable to attack by acid. Further, proton NMR titrations were employed to disclose the underlying mechanism. DMSO-*d6* with 1.2 M acids was added to $CDCl_3$ solution of BS-DPBDE (10 mM), ultimately with a volume ratio of 1: 100, circumventing the solvent effects on chemical shifts. The signals of proton 7, 8 and 9 are of non-movement under all tests, regarded as reference peak together with residual signal of $CDCl_3$ (**Fig. 3**c), signifying that Schiff-base backbone is stable in $CDCl_3$ with a small amount of acid although it might be unstable in acidic aqueous solution (Fig. S8). With gradual addition of HCl, the larger downfield shift of the dimethyl group proton 1 and aromatic protons 4 were observed, whereas the smaller downfield shift of that as replacing HCl with TFA. It is well-known that chemical shift is a measure of electron density near the proton being measured. And thus, it can be concluded that stronger acidic proton as electron acceptor makes protons 1 and 4 in BS-DPBDE deshielded heavily.[31] In contrast, proton 2 and 3 of the diethyl-amino group are less affected even though its high pKa value (N-diethylaniline, 6.56 vs N-dimethylaniline, 5.06[32]). The peaks appeared under addition of HCl to 0.8 equiv. (asterisk peaks) were contributed to slow-proton-exchange of protonated diethyl-amino group on the NMR time scale.[33]

3.4 Molecular mechanism and calculations.

To understand the fluorosolvatochromic behaviour, the fluorescence intensity of BS-DPBDE in different solvent with 1.5 equiv. HCl were associated with three solvatochromic parameters: polarity parameter ($E_T(30)$), hydrogen-bond-donating parameter (α), and hydrogen-bond-donating parameter (β) (Fig. 3b). It is apparent that no correlation is observed for $E_T(30)$ and α, whereas indicates that the fluorescence of BS-DPBDE is lighted up only in strong acid containing non-hydrogen-bond accepting solvents, choroform, whose β value approximate zero. Density functional theory (DFT) calculations revealed that the HOMOs, for both of BS-DPE and BS-DPBDE, are located on the donor-

acceptor diphenylpolyenes, whereas the LUMOs on the Schiff-base backbone (**Fig. 4** and **Table 3**). It is in sharp contrast with HOMO and LUMO of BS-Ph, both of which located on the Schiff-base backbone.[23] The non-superimposed HOMO and LUMO distribution support the photoinduced electron transfer (PET) process in these two molecules, which weakened and even quenched the fluorescence of the Schiff base backbone fluorophore. All of clues demonstrate that hydrogen-bond accepting solvents might enfeeble the electron withdrawing ability of acidic proton, and hence impeded the vanishment of PET process. We believe that this unique fluorescence phenomena might broaden our notion of fluorosolvatochromism and be applied in diverse fields.[34]

4. Conclusions

In closing, BSs derivatives, BS-DPE and BS-DPBDE, with two perpendicular ICT states have been synthesized and its spectroscopic and photophysical properties are described. We disclosed that boron in BSs as a node separated its two ICT states (Schiff base backbone ICT and diphenylpolyenes ICT states) and developed non-fluorescent PET compounds. Peculiarly, our work provides indisputable prerequisite for its fluorescent turn-on, that is, stronger acidic proton in non-hydrogen-bond accepting solvents. We believe that the unique fluorescence of BS-DPE and BS-DPBDE would not only spur new application in diverse field, but also provide the foundation for modification of conventional theories.

Acknowledgements

This work was supported by the Macao Science and Technology Development Fund under Grant No.: 052/2015/A2, 082/2016/A2, the Research Grant of University of Macau under grant No.: MYRG2016-00058-FHS, and MYRG2017-00066-FHS.

Appendix A. Supplementary data

Supplementary data related to this article can be found at

References

[1] Reichardt C, Welton T. Solvents and solvent effects in organic chemistry. 4th, updated and enl. ed. Weinheim, Germany: Wiley-VCH, 2011.

[2] Reichardt C. Solvatochromic Dyes as Solvent Polarity Indicators. Chem Rev 1994;94(8):2319-58.

[3] Shuai L, Luterbacher J. Organic Solvent Effects in Biomass Conversion Reactions. ChemSusChem 2016;9(2):133-55.

[4] Levy Y, Jortner J, Becker OM. Solvent effects on the energy landscapes and folding kinetics of polyalanine. Proc Natl Acad Sci U S A 2001;98(5):2188-93.

[5] LeGreve TA, James WH, 3rd, Zwier TS. Solvent effects on the conformational preferences of serotonin: serotonin-(H(2)O)(n), n = 1,2. J Phys Chem A 2009;113(2):399-410.

[6] Kosower EM. Mechanism of fast intramolecular electron-transfer reactions. J Am Chem Soc 1985;107(5):1114-8.

[7] Klymchenko AS. Solvatochromic and Fluorogenic Dyes as Environment-Sensitive Probes: Design and Biological Applications. Acc Chem Res 2017;50(2):366-75.

[8] Zhang R, Sun Y, Tian M, Zhang G, Feng R, Li X, et al. Phospholipid-Biomimetic Fluorescent Mitochondrial Probe with Ultrahigh Selectivity Enables In Situ and High-Fidelity Tissue Imaging. Anal Chem 2017;89(12):6575-82.

[9] Zamotaiev OM, Postupalenko VY, Shvadchak VV, Pivovarenko VG, Klymchenko AS, Mely Y. Monitoring penetratin interactions with lipid membranes and cell internalization using a new hydration-sensitive fluorescent probe. Org Biomol Chem 2014;12(36):7036-44.

[10] Mataga N, Kaifu Y, Koizumi M. Solvent Effects upon Fluorescence Spectra and the Dipolemoments of Excited Molecules. Bull Chem Soc Jpn 1956;29(4):465-70.

[11] Rathore R, Lindeman SV, Kochi JK. Charge-Transfer Probes for Molecular RecognitionviaSteric Hindrance in Donor-Acceptor Pairs. J Am Chem Soc 1997;119(40):9393-404.

[12] Rosokha SV, Kochi JK. Fresh look at electron-transfer mechanisms via the donor/acceptor bindings in the critical encounter complex. Acc Chem Res 2008;41(5):641-53.

[13] Lukinavicius G, Umezawa K, Olivier N, Honigmann A, Yang G, Plass T, et al. A near-infrared fluorophore for live-cell super-resolution microscopy of cellular proteins. Nat Chem 2013;5(2):132-9.

[14] Lukinavicius G, Reymond L, Umezawa K, Sallin O, D'Este E, Gottfert F, et al. Fluorogenic Probes for Multicolor Imaging in Living Cells. J Am Chem Soc 2016;138(30):9365-8.

[15] Dobretsov GE, Syrejschikova TI, Smolina NV. On mechanisms of fluorescence quenching by water. Biophysics 2014;59(2):183-8.

[16] Ghosh HN, Adamczyk K, Verma S, Dreyer J, Nibbering ET. On the role of hydrogen bonds in photoinduced electron-transfer dynamics between 9-fluorenone and amine solvents. Chem Eur J 2012;18(16):4930-7.

[17] Liu B, Shah M, Zhang G, Liu Q, Pang Y. Biocompatible flavone-based fluorogenic probes for quick wash-free mitochondrial imaging in living cells. ACS Appl Mater Interfaces 2014;6(23):21638-44.

[18] McDonald L, Liu B, Taraboletti A, Whiddon K, Shriver LP, Konopka M, et al. Fluorescent flavonoids for endoplasmic reticulum cell imaging. J Mater Chem B 2016;4(48):7902-8.

[19] Zhang B, Feng G, Wang S, Zhang X. Boronic acid derived salicylidenehydrazone complexes for wash-free fluorescence imaging of cellular organelles. Dyes Pigm 2018;149:356-62.

[20] DiCesare N, Lakowicz JR. Spectral Properties of Fluorophores Combining the Boronic Acid Group with Electron Donor or Withdrawing Groups. Implication in the Development of Fluorescence Probes for Saccharides. J Phys Chem A 2001;105(28):6834-40.

[21] Di Cesare N, Lakowicz JR. Wavelength-ratiometric probes for saccharides based on donor–acceptor diphenylpolyenes. J Photochem Photobiol, A 2001;143(1):39-47.

[22] DiCesare N, Lakowicz JR. New sensitive and selective fluorescent probes for fluoride using boronic acids. Anal Biochem 2002;301(1):111-6.

[23] Santos FM, Rosa JN, Candeias NR, Carvalho CP, Matos AI, Ventura AE, et al. A Three-Component Assembly Promoted by Boronic Acids Delivers a Modular Fluorophore Platform (BASHY Dyes). Chem Eur J 2016;22(5):1631-7.

[24] Alcaide MM, Santos FMF, Pais VF, Carvalho JI, Collado D, Perez-Inestrosa E, et al. Electronic and Functional Scope of Boronic Acid Derived Salicylidenehydrazone (BASHY) Complexes as Fluorescent Dyes. J Org Chem 2017;82(14):7151-8.

[25] Adhikari RM, Shah BK, Palayangoda SS, Neckers DC. Solvent dependent optical switching in carbazole-based fluorescent nanoparticles. Langmuir 2009;25(4):2402-6.

[26] Hoang CT, Prokes I, Clarkson GJ, Rowland MJ, Tucker JH, Shipman M, et al. Study of boron-nitrogen dative bonds using azetidine inversion dynamics. Chem Commun 2013;49(25):2509-11.

[27] Shinmori H, Takeuchi M, Shinkai S. Spectroscopic sugar sensing by a stilbene derivative with push (Me2N-)-pull ((HO)2B-)-type substituents. Tetrahedron 1995;51(7):1893-902.

[28] Clover AM. The Auto-Oxidation of Chloroform. J Am Chem Soc 1923;45(12):3133-8.

[29] Lakowicz JR. Principles of fluorescence spectroscopy. 3rd ed. New York: Springer, 2006.

[30] Ghosh P, Das T, Maity A, Purkayastha P. Light induced dynamics of a charge transfer probe in lipid vesicles. Soft Matter 2012;8(39):10178.

[31] Perruchoud LH, Jones MD, Sutrisno A, Zamble DB, Simpson AJ, Zhang Xa. A ratiometric NMR pH sensing strategy based on a slow-proton-exchange (SPE) mechanism. Chem Sci 2015;6(11):6305-11.

[32] Hall NF, Sprinkle MR. Relations between the Structure and Strength of Certain Organic Bases in Aqueous Solution. J Am Chem Soc 1932;54(9):3469-85.

[33] Bryant RG. The NMR time scale. J Chem Educ 1983;60(11):933.

[34] Lee J, Chang HT, An H, Ahn S, Shim J, Kim JM. A protective layer approach to solvatochromic sensors. Nat Commun 2013;4:2461.

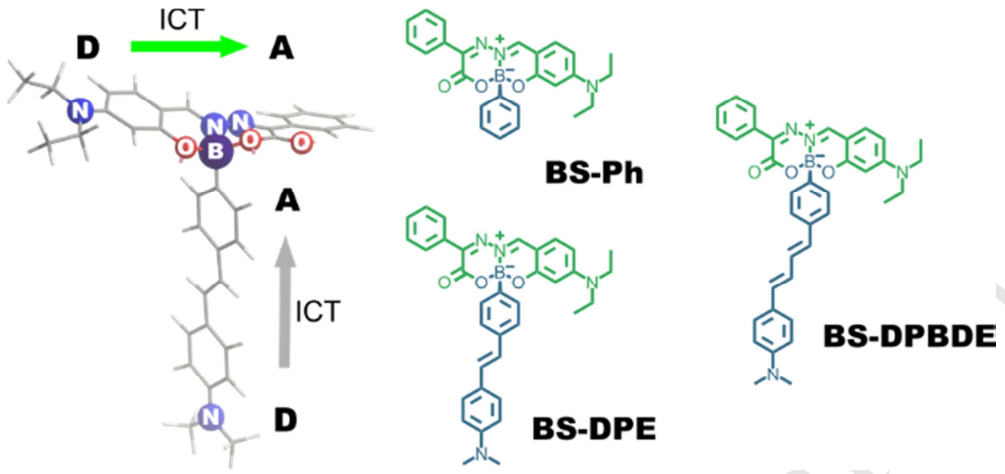

Scheme 1 T-shape molecular geometry of BSs with two perpendicular ICT states (The DFT optimized structure) and the structures of BS-Ph, BS-DMA, BS-DPE and BS-DPBDE

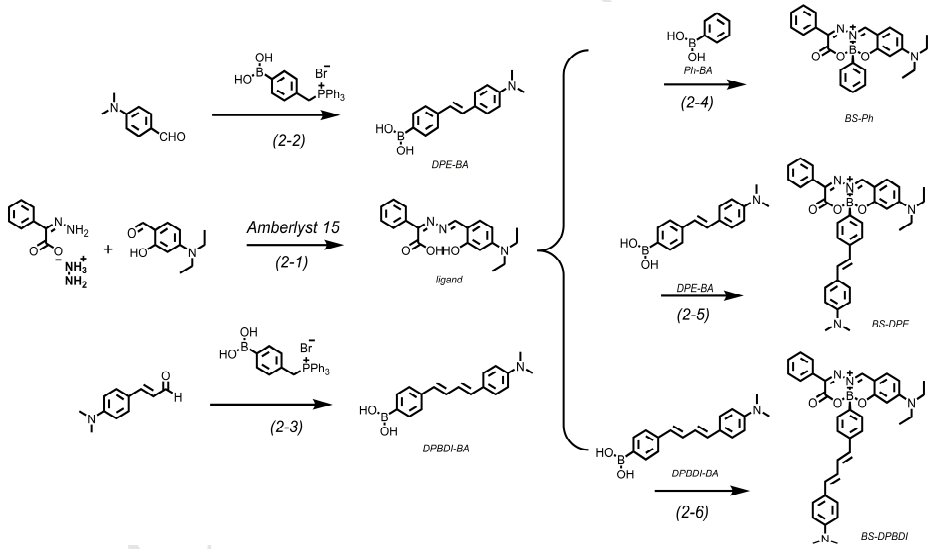

Scheme 2 Synthetic routine of BS-Ph, BS-DPE and BS-DPBDE

Table 1 Spectral Properties and Fluorescence Quantum Yield (Φ_s) of the BS-DPE and BS-DPBDE in different solvents.

Compd	solvent	λ_{abs} (nm)		ε ($M^{-1}cm^{-1}$)	λ_{em}[b] (nm)	Δ[c] (nm)	Φ_s
BS-DPE	$CDCl_3$	321	478	53000	518	40	0.43
	$CHCl_3$	357	478	52000	517	39	<0.01
	CH_2Cl_2	359	477	52000	522	45	<0.01
	Toluene	355	472	54000	508	36	<0.01
	THF	355	471	55000	517	46	<0.01
	PEG400	361	478	43000	535	57	<0.01
	DMSO	363	478	42000	552	74	<0.01
	CH_3OH	351	473	43000	537	64	<0.01
	20 mM HEPES	356	471	38000	—[a]		
BS-DPBDE	$CDCl_3$	344	469	58000	518	49	0.52
	$CHCl_3$	387	478	56000	517	39	0.02
	CH_2Cl_2	390	477	55000	522	45	0.02
	Toluene	387	472	59000	509	37	0.02
	THF	384	472	55000	520	48	<0.01
	PEG400	387	477	48000	533	56	<0.01
	DMSO	386	479	47000	544	65	<0.01
	CH_3OH	379	473	46000	553	80	<0.01
	20 mM HEPES	389	465	40000	—[a]		

[a] Not determined due to the weak fluorescence. [b] λ_{ex} = at 470 nm. [c] Stokes shift.

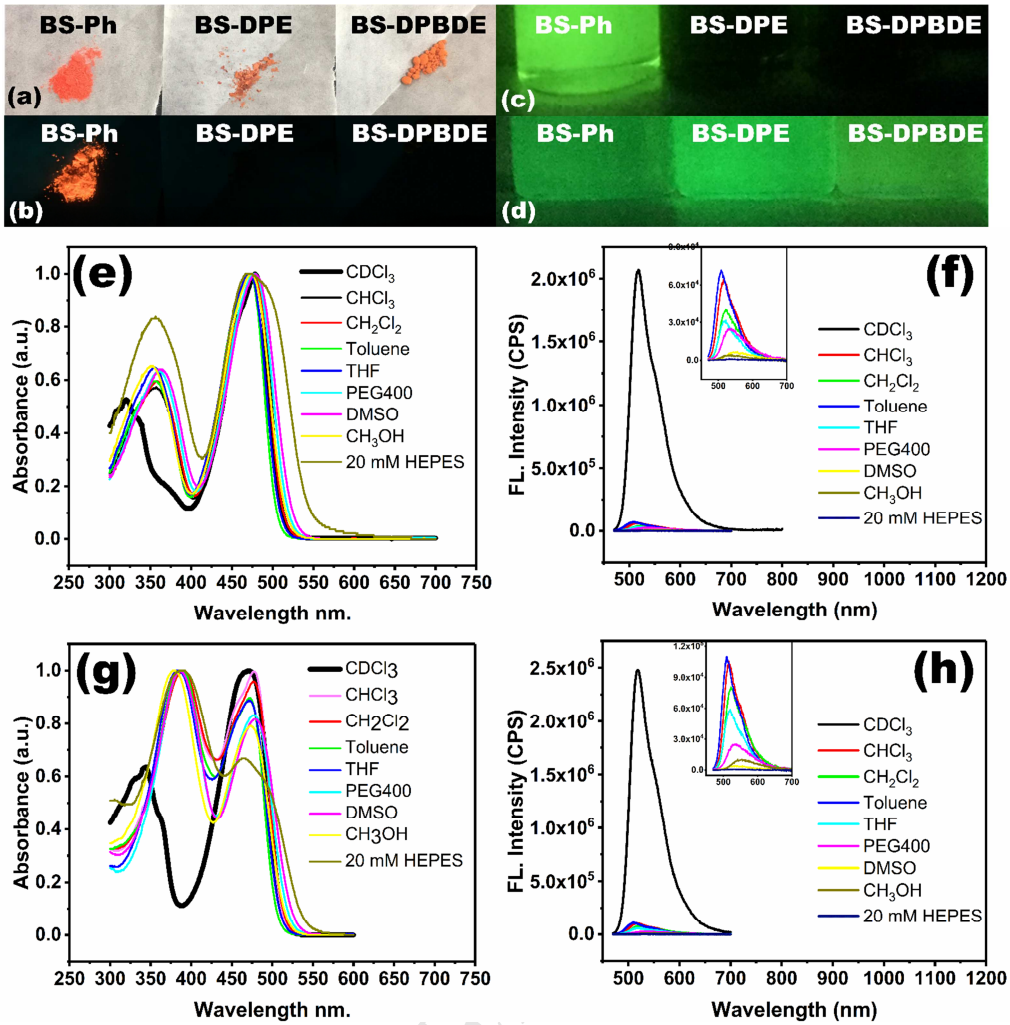

Fig. 1 Image of compounds BS-Ph, BS-DPE and BS-DPBDE (a) under vis light; (b) in solid states, (c) dissolved in $CHCl_3$ or (d) in $CDCl_3$ under 365 nm UV light. Absorption (e, g) and emission spectra (f, h) of BS-DPE (e, f) and BS-DPBDE (10 uM) (g, h) in $CDCl_3$, $CHCl_3$, CH_2Cl_2, toluene, THF, PEG400, DMSO, CH_3OH and HEPES buffer (20 mM). (excitation at 450 nm, slit: 1 nm/1 nm)

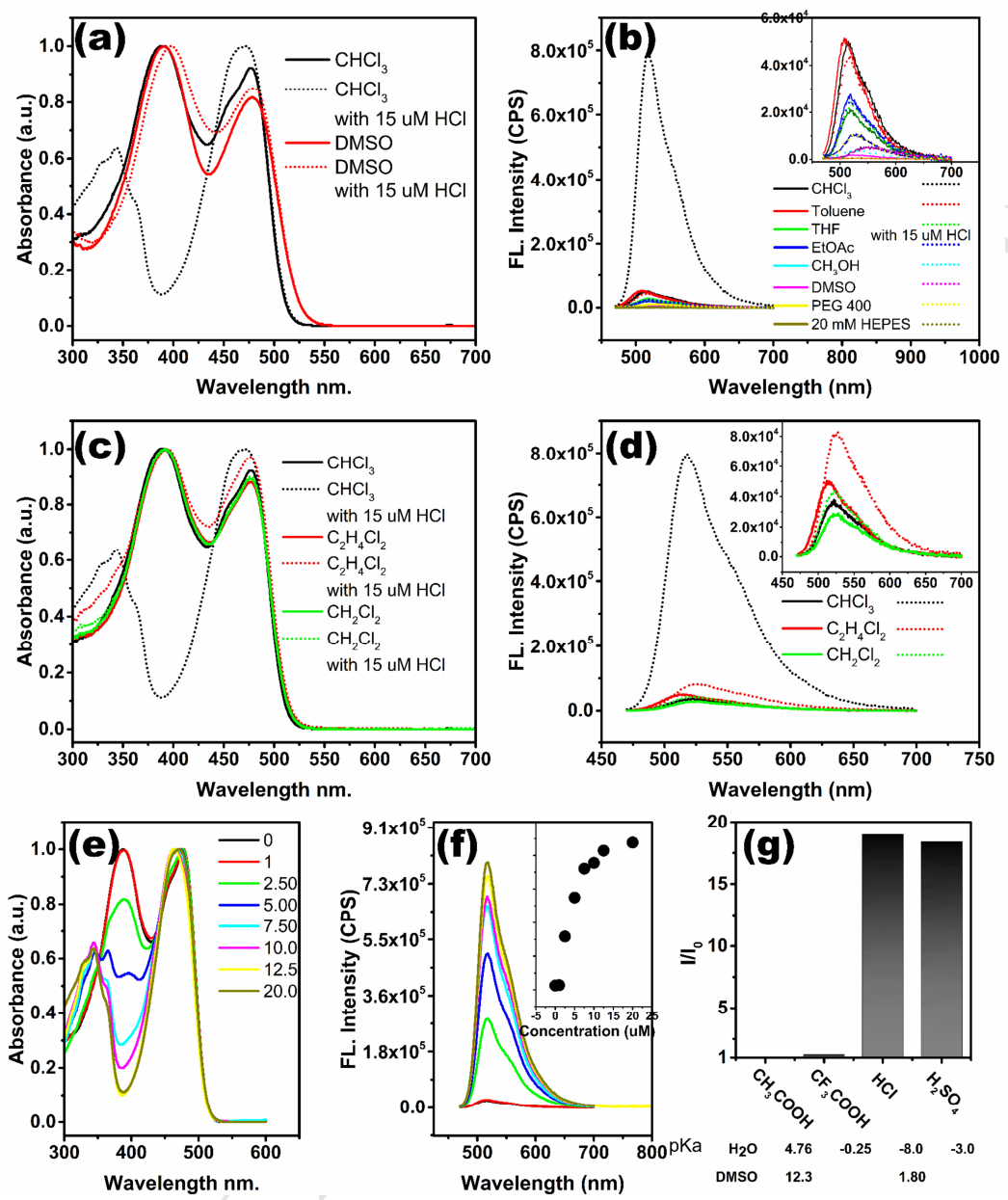

Fig. 2 Absorption (a, c) and emission (b, d) spectra of 10 uM BS-DPBDE in different solvents with or without 15 uM HCl. Notes: for (b), $CHCl_3$ (black), toluene (red), THF (green), EtOAc (blue), CH_3OH (cyan), DMSO (magenta), PEG400 (yellow) and 20 mM HEPES buffer (dark yellow); short dot line, with 15 uM HCl. Absorption (e) and emission (f) titration spectra in the presence of varying concentrations of HCl in $CHCl_3$. (g) the emission ratio (I/I_0) upon adding acid into $CHCl_3$ solution. (excitation at 450 nm, slit: 1 nm/1 nm)

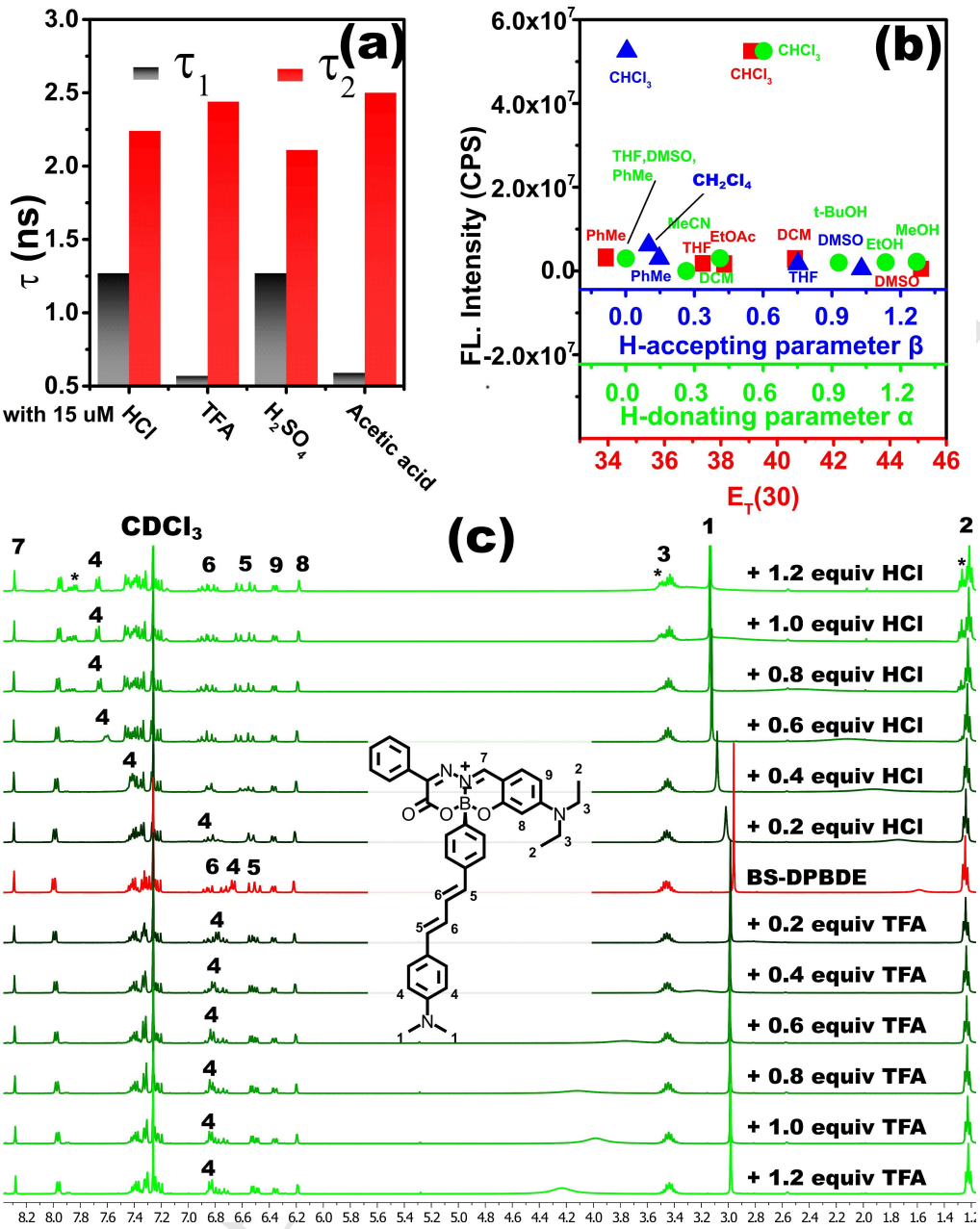

Fig. 3 (a) The distribution of fluorescence decay times of BS-DPBDE in $CHCl_3$ with 15 uM acids (BS-DPBDE, 10 uM), data from **Table 2** and Fig S3-4 (b) Relationship between the fluorescent intensity of BS-DPBDE in 15 uM HCl solution and the solvatochromic parameters ET(30), hydrogen-bond-donating parameter (α), and hydrogen-bond-accepting parameter (β) of solvents. Partial Data are repeated from Fig.2; (c) ^{1}H NMR titration of BS-DPBDE with HCl and TFA in $CDCl_3$ (BS-DPBDE, 10 mM).

379

Table 2 Fluorescence Decay Parameters of the BS-DPBDE investigated in different solvent with or without acid

		τ_1 (ns)	τ_2 (ns)	α_1	α_2	$\bar{\tau}$ (ns)	χ_R^2
1	$CHCl_3$	0.60	2.45	0.18	0.82	2.36	1.7
2	$CHCl_3$ with 15 uM HCl	1.27	2.24	0.18	0.82	2.13	1.9
3	CH_2Cl_2	0.74	2.41	0.32	0.68	2.20	1.9
4	CH_2Cl_2 with 15 uM HCl	0.64	2.22	0.38	0.62	1.98	1.7
5	Toluene	0.90	2.23	0.20	0.80	2.11	1.6
6	Toluene with 15 uM HCl	0.87	2.10	0.39	0.61	1.84	1.6
7	THF	0.05	1.25	0.26	0.74	1.23	3.8
8	THF with 15 uM HCl	0.09	1.06	0.22	0.78	1.04	6.0
9	DMSO	0.34	0.80	0.62	0.38	0.61	2.0
10	DMSO with 15 uM HCl	0.51	2.24	0.97	0.03	0.72	2.6
11	$CHCl_3$ with 15 uM TFA	0.57	2.44	0.26	0.74	2.30	1.5
12	$CHCl_3$ +15 uM H_2SO_4	1.27	2.11	0.42	0.58	1.86	1.6
13	$CHCl_3$ +15 uM Acetic acid	0.59	2.50	0.17	0.83	2.41	1.8

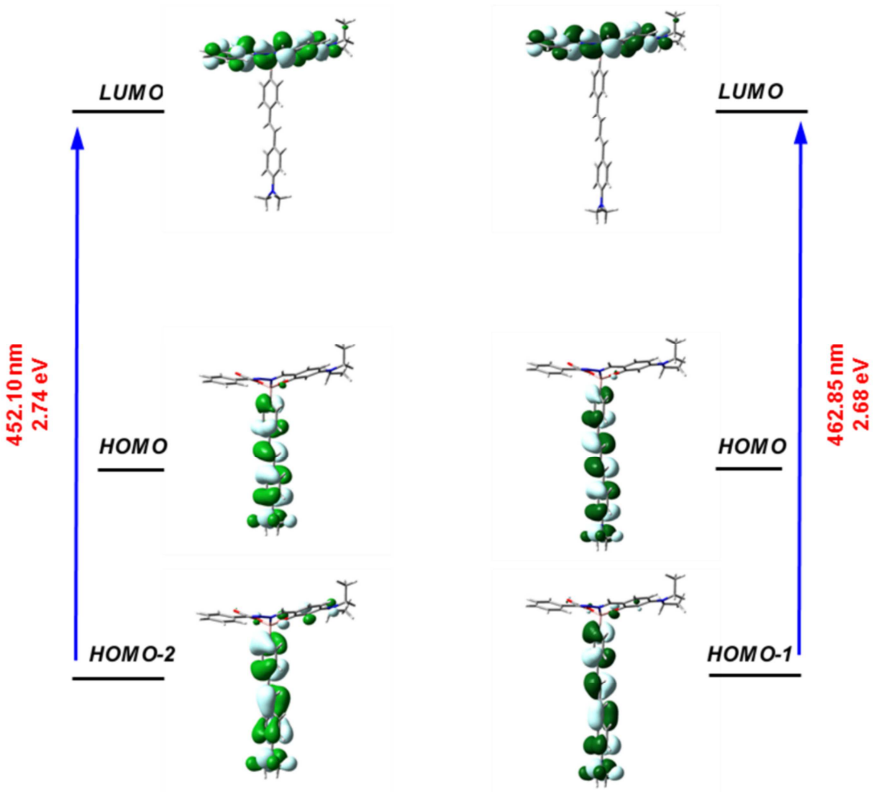

Fig. 4 Molecular orbitals (LUMO and HOMO) and HOMO/LUMO energy gaps of BS-DPE and BS-DPBDE.

Table 3 Calculated single-photon related spectral properties of BS-DPE, BS-DPBDE in the gas phase.

Comp.	λ_{max}(nm) [a]	ΔE_1(eV) [b]	f	OI [c]
	452.10	2.74	0.1196	149 → 152 (H-2 → L)
2	462.85	2.68	0.0296	157 → 159 (H-1 → L)

a. Peak position of the longest absorption band; *b.* The energy gap of the one-photon absorption band; *c.* TD-DFT method with the orbitals Involved (OI).

Highlights

- Two boronic acid derived salicylidenehydrazone complexes (BSs) with two perpendicular ICT states, BS-DPE and BS-DPBDE, were synthesized and characterized.
- The non-fluorescent PET characteristic of BS-DPE and BS-DPBDE were disclosed.
- Relative strong acidic proton in non-hydrogen-bond accepting solvent were proved to actuate the vanishment of PET and reinstatement of its fluorescence.